

## MICRO-TYPE III RADIO BURSTS

AKIRA MORIOKA,<sup>1</sup> YOSHIZUMI MIYOSHI,<sup>2</sup> SATOSHI MASUDA,<sup>2</sup> FUMINORI TSUCHIYA,<sup>1</sup> HIROAKI MISAWA,<sup>1</sup>  
HIROSHI MATSUMOTO,<sup>3</sup> KOZO HASHIMOTO,<sup>4</sup> AND HIROSHI OYA<sup>5</sup>

Received 2006 July 3; accepted 2006 October 24

### ABSTRACT

We present a detailed description of the features of solar “micro-type III” radio bursts, which are elements of the so-called type III storms, using long-term observations made by the *Geotail* and *Akebono* satellites. Micro-type III bursts are characterized by short-lived, continuous, and weak emission. Their average power is estimated to be well below that of the largest type III bursts, by 6 orders of magnitude. When they occur, these bursts have a distribution of emitted power flux that is different from that of ordinary type III bursts, indicating that they are not just weaker versions of the ordinary bursts. Micro-type III burst activity is not accompanied by significant solar soft X-ray activity. We identify the active regions responsible for micro-type III bursts by examining the concurrence of their development and decay with the bursts. It is found that both micro and ordinary type III bursts can emanate from the same active region without interference, indicating the coexistence of independent electron acceleration processes. It is suggested that the active regions responsible for micro-type III bursts generally border on coronal holes.

*Subject headings:* Sun: activity — Sun: corona — Sun: radio radiation

### 1. INTRODUCTION

Solar type III bursts are one of the typical radio emissions associated with flares, being produced by electron beams traveling along the coronal and interplanetary magnetic field lines. By making use of the observed wave characteristics of these bursts, various studies have been carried out on (1) the acceleration and dynamics of nonthermal electrons (e.g., Lin et al. 1981; Klein et al. 2005; Simnett 2005), (2) the excitation of plasma waves by nonthermal electrons and the propagation of radio waves in the solar corona and interplanetary space (e.g., Wild et al. 1963; Gumett & Anderson 1976; Dulk et al. 1998; Ergun et al. 1998), and (3) the plasma environment in the coronal and interplanetary medium (e.g., Fainberg & Stone 1971; Leblanc et al. 1998; Reiner 2001).

Using observations from the *RAE 1* satellite, Fainberg & Stone (1970a, 1970b, 1971, 1974) demonstrated the existence of radio storm phenomena that are characterized by thousands of bursts lasting for several days in the hectometric and kilometric wavelength ranges. They noted that this particular phenomenon is distinctly different from individual or grouped type III bursts because of their long duration and referred to them as a “‘storm’ of type III bursts.” The *ISEE 3* interplanetary observations detected many such storms, and their statistical features and relationship to solar activity were elucidated by Bougeret et al. (1984a, 1984b). From these satellite observations, extensive information on the bursts’ fundamental characteristics has been derived (Fainberg & Stone, 1970a, 1970b, 1971, 1974; Bougeret et al. 1984a, 1984b). The storms are often observed for half a solar rotation and occasionally last for more than a full rotation; such a sustained occurrence of bursts implies a quasi-continuous injection of nonthermal electrons into interplanetary space from solar active regions. The average speed of these electron beams has been estimated from

the rate at which the emissions drift in frequency. The type III “storms” appear with lower intensity and in a limited frequency range compared with ordinary type III emissions. It has been suggested that the burst activity may be correlated with daily sunspot numbers in the short term and with the solar cycle over the long term. The height of the acceleration region of the nonthermal electrons has been inferred to be less than  $2 R_{\odot}$  based on the correlation between metric type III and type I storms.

Basically, the excitation process for the individual components of a type III storm might be expected to be similar to that for an ordinary type III burst. The nonthermal electron beams, which are accelerated around active regions and injected along field lines, excite Langmuir waves at the local plasma frequency. Part of the energy of these Langmuir waves is then converted into radio waves through a nonlinear process. The frequency of these waves will drift as the electron beam moves outward into the interplanetary medium. However, the most prominent feature of type III storms, that is, continuous emission of thousands of short-lived bursts having weak intensities over a prolonged period, seems to indicate source characteristics that are different from that of ordinary type III bursts.

We consider the term “type III storm” inadequate in discussing the source characteristics of the individual components of such events. Instead, in this paper we will use the term “micro-type III burst” to refer to the constituent elements of a type III storm.

One of the most interesting issues surrounding these micro-type III bursts is their relation to microflares, X-ray jets, and similar solar phenomena. Lin et al. (1984) found “microflares” in hard X-rays that are 6 orders of magnitude smaller than the largest flares. “Small-scale brightenings” in the extreme-ultraviolet (Porter et al. 1987, 1995) and “transient brightenings” in soft X-rays (Shimizu et al. 1992, 1994) have been reported and discussed from the viewpoint of coronal heating by microflares (Hudson 1991). Liu et al. (2004) demonstrated that microflare events observed by the satellite *RHESSI* were associated with type III bursts detected by the *Wind* spacecraft. Solar X-ray jets associated with small flares were observed by the *Yohkoh* satellite (Shibata et al. 1992). A detailed study of the characteristics of micro-type III bursts should lead to a better understanding of the microscale processes that accelerate the electron beam.

<sup>1</sup> Planetary Plasma and Atmospheric Research Center, Tohoku University, Sendai, Miyagi, Japan.

<sup>2</sup> Solar-Terrestrial Environment Laboratory, Nagoya University, Nagoya, Aichi, Japan.

<sup>3</sup> Kyoto University, Kyoto, Japan.

<sup>4</sup> Research Institute for Sustainable Humanosphere, Kyoto University, Uji, Kyoto, Japan.

<sup>5</sup> Department of Space Communication Engineering, Fukui University of Technology, Fukui City, Fukui, Japan.

The purpose of this paper is (1) to characterize the occurrence of micro-type III bursts in detail, from long-term radio-wave observations made by the *Akebono* and *Geotail* satellites, and to compare them with the results of earlier, pioneering studies; (2) to investigate whether these bursts are generated through the same process as ordinary type III bursts; and (3) to determine the characteristics of the active regions that are responsible for the micro-type III bursts.

## 2. OBSERVATIONS AND DATA

The solar radio emission data were obtained from the *Geotail* and *Akebono* satellites. *Geotail*, which has an eccentric equatorial orbit, was launched in 1992. Since then, it has been carrying out detailed measurements of plasma and electromagnetic phenomena in the magnetosphere and interplanetary space. The Plasma Wave Instrument (PWI; Matsumoto et al. 1994) on board the spacecraft observes plasma and radio waves from 5.6 Hz to 800 kHz and provides spectral data with a time resolution of 8 s in a frequency range from 24 Hz to 800 kHz. These observations are useful for statistical analysis, as we have almost complete data coverage since the launch of the satellite. *Akebono* was launched in 1989 into a polar orbit with an initial apogee height of 10,500 km. Its Plasma Wave and Sounder instrument (PWS; Oya et al. 1990) provides observational data on terrestrial and extraterrestrial plasma and radio waves from 20 kHz to 5 MHz with a time resolution of 2 s. The spin axis of the spacecraft is Sun-oriented, so that the solar radio emissions received by its orthogonal dipole antennas are free from spin modulation. The data coverage was restricted to 40%–60% of each day, depending on the distribution of tracking stations. Because of their high time resolution and wide frequency range, the *Akebono* data are useful for detailed spectral analysis of solar radiation.

Solar X-ray data from the *Yohkoh* satellite (Ogawara et al. 1991) were used to monitor solar activity. The Nobeyama Radio Heliograph was used at 17 GHz as a reference for the solar radio active region. The active region data from the SolarMonitor site at Goddard Space Flight Center's Solar Data Analysis Center were used to identify the active regions responsible for the burst phenomena.

## 3. DYNAMIC SPECTRA OF MICRO-TYPE III BURSTS

Figure 1 shows sample spectrograms of solar type III bursts in the kilometric wavelength range (10–800 kHz) as observed by *Geotail*. The 24 hr spectrogram in the top panel shows a very large type III burst that was detected around 10:20 UT on 2000 July 14. The duration of this burst was well over 7 hr in its lower frequency components. The discontinuity in frequency drift at 100 kHz is caused by the different frequency sweep rates of the receiver between the lower (10–100 kHz; 90 kHz per 8 s) and higher (100–800 kHz; 700 kHz per 8 s) bands. The lower cutoff frequency of the burst was found to be same as the local plasma frequency at the spacecraft's location, indicating that the solar electron beam was passing through 1 AU. This large type III burst coincided with an X5.7 flare in the solar northern hemisphere (N22°, W07°), the so-called Bastille Day event. It should be noted that the intense signals seen in the frequency band from 100 to 500 kHz during the first 3 hr in this spectrogram are auroral kilometric radiation (AKR) from the terrestrial auroral region.

A type III burst associated with an M-class flare is shown in Figure 1b; the burst was detected around 07:00 UT on 1999 June 4. Its duration was 2 hr or more in the lower frequency band, below 100 kHz. Many type III bursts of rather weak intensity and shorter duration were observed intermittently on the same day. In this

paper, we refer to the discrete type III bursts shown in these two panels as “ordinary type III bursts.”

Figures 1c and 1e show sequences of very fine solar bursts. Radiation above ~200 kHz resembling continuous wideband emission occurred throughout the days of 2001 May 23 (Fig. 1c) and 2003 October 23 (Fig. 1e). A group made up of thousands of such bursts is what is referred to as a “storm” of type III bursts (Fainberg & Stone 1970a). The expanded spectrograms shown in Figures 1d and 1f indicate that this emission is made up of a sequence of fine type III bursts (micro-type III bursts). All these bursts above 200 kHz show a pattern of frequency drift similar to that of ordinary type III bursts. However, it should be noted from this comparison that the micro-type III bursts can be characterized as having (1) a very low intensity, as can be inferred roughly from the color-coded intensity scale (about 50 dB lower than large type III bursts); (2) short durations, of less than a few minutes; (3) a relatively higher cutoff frequency (about 200 kHz); and (4) continuity (they last for many hours).

## 4. CHARACTERISTICS OF MICRO-TYPE III BURSTS

### 4.1. Radiation Power

To estimate the power in the observed radio emissions, we use data from observations made by the *Akebono* satellite, which have 2 s time resolution and no spin modulation. Figure 2 shows intensity profiles at 1.34 MHz of the type III burst associated with the X5.7 flare shown in Figure 1a and the micro-type III bursts shown in Figure 1d. Integrating the intensity profiles over time, we estimate the power of the type III burst associated with the X5.7 flare (duration of 45 minutes) to be  $1.6 \times 10^{-10} \text{ V}^2 \text{ m}^{-2} \text{ Hz}^{-1} \text{ s}$  (Fig. 2a). On the other hand, the sampled micro-type III burst (Fig. 2b, *asterisk*) has a power of  $1.7 \times 10^{-15} \text{ V}^2 \text{ m}^{-2} \text{ Hz}^{-1} \text{ s}$  for its 1 minute duration. The ratio in power of the micro-type III burst to the type III burst associated with the X5.7 flare is thus  $\sim 10^{-5}$ . For the largest type III bursts, associated with X10 class flares, the corresponding ratio in power would be well below  $10^{-6}$ . Thus, the term “micro-type III” can be justified in terms of their observed power.

### 4.2. Power Distribution

We have carried out a statistical investigation of the distribution of power in type III bursts, including micro-type III, using long-term *Akebono* observations covering four Bartels rotations (BR 2255, 2264, 2265, 2275). The total duration of observations was 675.7 hr (data for the period when the AKR activity expanded to over 800 kHz and when the spacecraft was in the shadow of Earth were excluded). During this period, there were many ordinary type III bursts and some groups of micro-type III bursts (so-called type III storms). To investigate the distribution of type III bursts with respect to flux density, profiles of intensity versus time at certain frequencies were first low-pass filtered to remove background fluctuations. This was followed by further processing with an automated peak detection algorithm. The results are shown in Figure 3 for the cases of 860 kHz (*top*) and 1.34 MHz (*bottom*). These distributions can be fitted with two different power laws. The lines with the steeper slope dominate in the region of lower flux density and have power-law indices of 3.61 at 860 kHz and 3.68 at 1.34 MHz. The lines with the slowly varying slope extend to higher flux densities and have power-law indices of 0.52 at 860 kHz and 0.69 at 1.34 MHz. The steeper lines show the occurrence distribution of micro-type III bursts with respect to the flux density, and the shallower ones show the distribution of the ordinary type III bursts. These distinct distributions lead to an important conclusion: the ordinary type III and the micro-type III

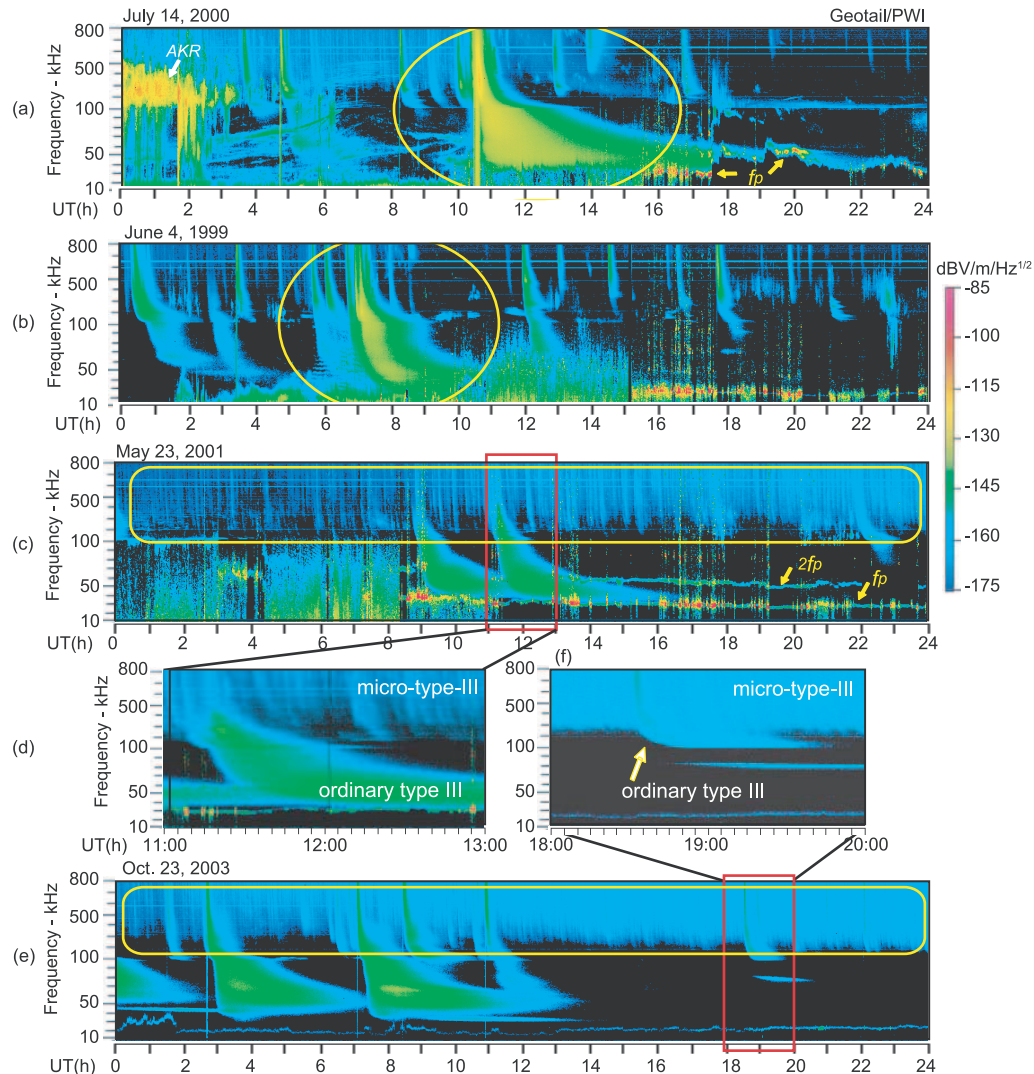


FIG. 1.—Sample 24 hr dynamic spectrograms of electric field in the frequency range from 10 to 800 kHz as observed by the *Geotail* satellite. The frequency sweep rate of the receiver is different in the low (10–100 kHz) and high (100–800 kHz) bands. (a) Dynamic spectrogram from 2000 July 14. (b) Dynamic spectrogram from 1999 June 4. (c) Dynamic spectrogram from 2001 May 23; the emissions above  $\sim 200$  kHz are a train of micro-type III bursts. (d) Expanded view of (c) for the period from 11:00 to 13:00 UT. (e) Dynamic spectrogram from 2003 October 23. Emissions above about 200 kHz are again a train of micro-type III bursts. (f) Expanded view of (e) for the period from 18:00 to 20:00 UT.

bursts have different sources and may have different electron acceleration processes.

#### 4.3. Recurrence

One of the most striking features of the micro-type III bursts that distinguishes them from ordinary type III bursts is that they are continuous and last for many days, as first shown by Fainberg & Stone (1970a). In this study, the occurrence characteristics of micro-type III bursts are studied in detail using long-term data from *Geotail*. Figure 4 shows dynamic spectrograms for the period from 2001 March 2 to May 21 in the 10–800 kHz frequency range. These spectrograms are arranged in order of Bartels rotation, from BR 2288 to BR 2290. The rather intense signals centered around 200–300 kHz, occasionally extending to lower frequencies, are AKR. The frequency components below 50 kHz are either terrestrial or interplanetary plasma waves, depending on the location of the spacecraft. The burstlike spectra extending from 800 kHz to below 100 kHz are ordinary type III bursts. The micro-type III bursts appear as continuous wideband emissions in the fre-

quency range between  $\sim 100$  and 800 kHz—that is, the light blue spectra shown in the diagrams and enclosed by rectangles. It should be noted that the continuous micro-type III bursts arise late in each Bartels rotation and continue until the early stages of the next rotation, reappearing for at least three rotations as shown in Figure 4. Figure 5 shows radio heliograms at 17 GHz from Nobeyama Radio Observatory during the period from 2001 March 17 to April 5. Comparing with Figure 4, one can see that the rise of the radio active region from the eastern limb (*yellow arrows*) on March 23 is almost correlated with the beginning of the continuous micro-type III bursts, and that the set of radio active regions in the western limb on April 3 coincided with the absence of the continuous micro-type III bursts. This suggests that a particular active region was responsible for the generation of the series of micro-type III bursts, as observed in earlier studies (Fainberg & Stone 1970a; Bougeret et al. 1984a).

Another interesting characteristic of the micro-type III bursts is that their cutoff frequency is always above 100 kHz. This can be seen from the long-term spectrograms in Figure 4.

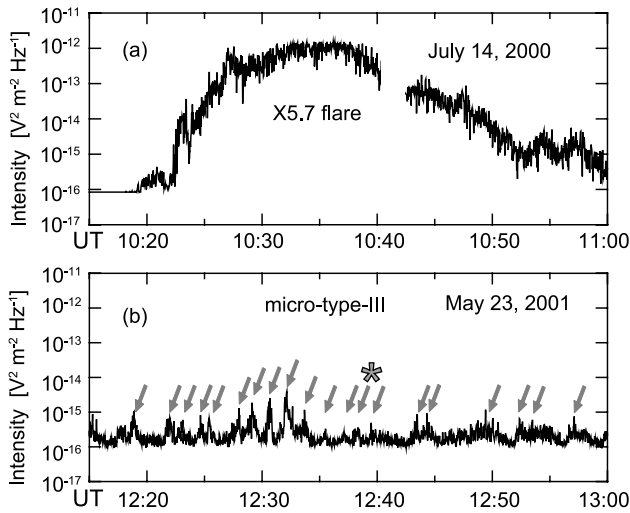


FIG. 2.—Intensity profile at 1.34 MHz for (a) the large type III burst shown in Fig. 1a and (b) micro-type III bursts corresponding to Fig. 1d. The arrows in (b) indicate the bursts. The asterisk indicates the micro-type III burst whose power is estimated in the text.

#### 4.4. Short-Term Occurrence Rate

Usually, micro-type III bursts appear repeatedly, as originally pointed out by Fainberg & Stone (1974). We examined the typical short-term occurrence rate by counting the number of bursts in the dynamic spectrograms, making use of an automated burst detection algorithm. Figure 6 shows the detailed dynamic spectrogram in the frequency range from 380 kHz to 5.28 MHz observed on 2001 May 23 by the *Akebono* satellite. *Akebono* was located above the polar ionosphere at an altitude of about 6800 km. During these 30 minutes, a total of 24 micro-type III bursts were detected, which equates to an approximate occurrence rate of 50 bursts per hour. The algorithm also found 180 bursts per hour for a violent micro-type III storm on 1999 July 4. Thus, the typical short-term occurrence rate can be estimated to be roughly 50–200 events per hour on an active day. It should be noted that the cutoff frequency of  $\sim 500$  kHz seen in Figure 6 is not real, but a result of propagation effects on solar radio waves in the near-Earth magnetosphere.

#### 4.5. Relationship with Solar Activity

To evaluate the daily occurrence frequency of micro-type III bursts, we introduce a “micro-type III burst index” (hereafter the “mt-III index”). The corresponding levels express the duration of occurrence of micro-type III bursts during a 24 hr long dynamic spectrogram: “1,” “2,” and “3” correspond to “less than one-third of a day,” “less than half a day,” and “all day long,” respectively. The long-term activity represented by the index is shown in Figure 7 for the period from 1997 October 7 (BR 2242) to 2005 November 23 (BR 2351) with respect to the solar rotation. It can be seen that continuous micro-type III bursts are a rather common phenomenon, as pointed out by Fainberg & Stone (1970a). The average duration is about 5 days, which is consistent with the early results of Bougeret et al. (1984a). The recurring appearance with solar rotation is also found to be frequent, indicating that the active regions responsible for the micro-type III bursts are long-lived. Sometimes they continue for more than four solar rotations, as can be seen in 1999, 2001, and 2002.

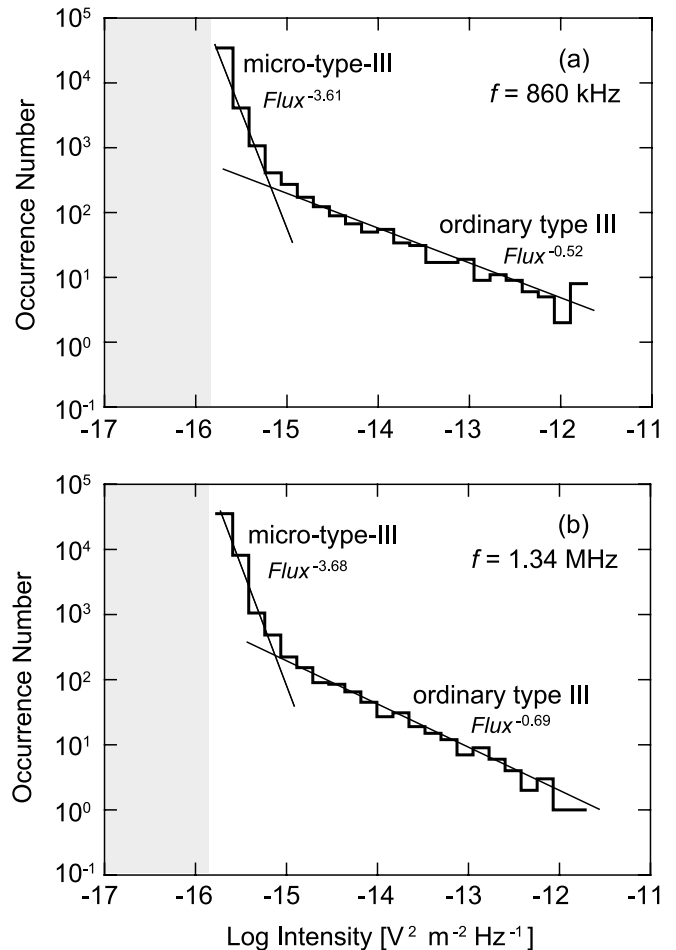


FIG. 3.—Distribution of type III bursts with respect to flux intensity at (a) 860 kHz and (b) 1.34 MHz. Their occurrence can be seen to obey two distinct power laws. The shaded area indicates the region limited by sensitivity of the receiver.

The relationship between the activity of micro-type III bursts and the solar cycle was also investigated. Figure 8 (*top*) shows a plot of the integrated daily mt-III index ( $\sum$  mt-III), which is the sum of individual daily mt-III indices for a solar rotation. Although the sum (*black line*) seems to fluctuate in a random manner from rotation to rotation, its average trend (*gray line*) indicates a weak correlation with variations in sunspot number during the solar cycle (*bottom*). This result is thus slightly different from the earlier investigation carried out by Bougeret et al. (1984a), where a solar cycle dependence of type III storm intensity was suggested.

#### 4.6. Relationship with GOES X-Rays

Major flares are usually accompanied by soft X-ray bursts and ordinary type III radio bursts. It has been confirmed that microflares are associated with the weak soft X-rays and also with type III radio bursts (Shimizu et al. 1992; Liu et al. 2004). The question here is whether micro-type III bursts are accompanied by soft X-ray events. Figure 9 illustrates the relationship between micro-type III bursts observed by *Geotail* and soft X-rays as observed by *GOES 10*. The micro-type III bursts appeared continuously above 200 kHz during the 2 days shown. However, the X-ray data do not show any particular enhancement corresponding to micro-type III burst activity, except for transient pulses, with flux levels below  $10^{-8} W m^{-2}$ .

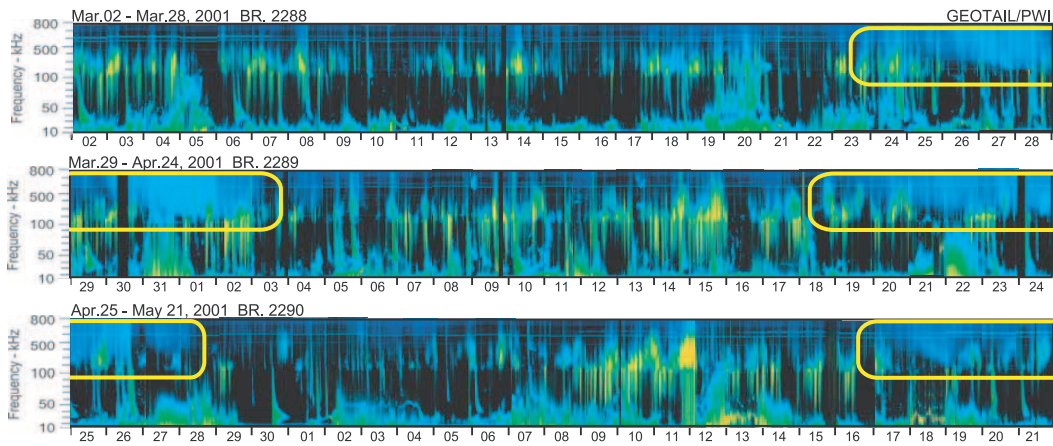


FIG. 4.—Long-term dynamic spectrograms arranged with respect to Bartels rotation, from BR 2288 to BR 2290. The yellow outlines show the recurrent appearance of continuous micro-type III bursts. The intense signals seen from  $\sim 100$  to  $\sim 500$  kHz are auroral kilometric radiation (AKR).

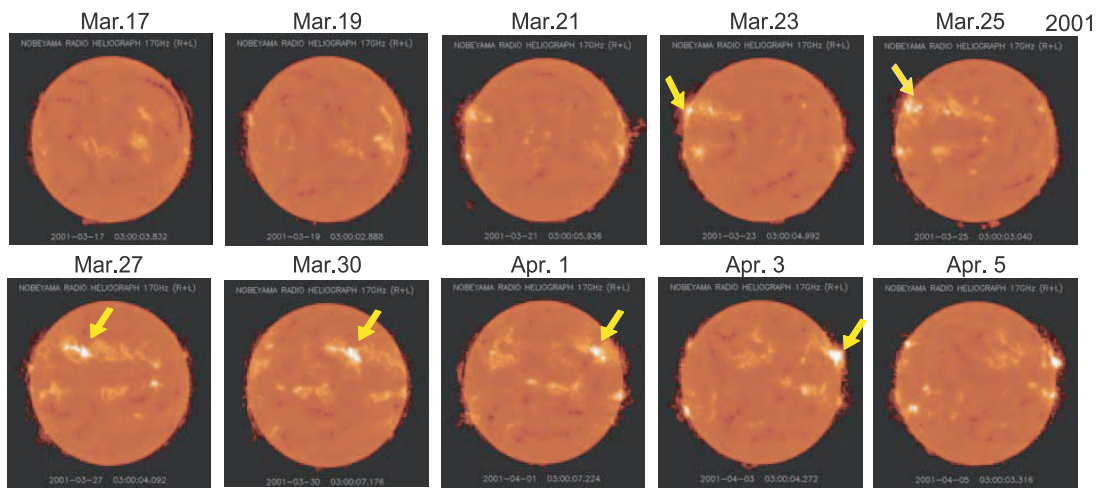


FIG. 5.—Radio image at 17 GHz from the Nobeyama Radio Heliograph for the period from 2001 March 17 to April 5. The arrows show the active region responsible for the micro-type III bursts observed in Bartels rotations 2288–2289 that are shown in Fig. 4.

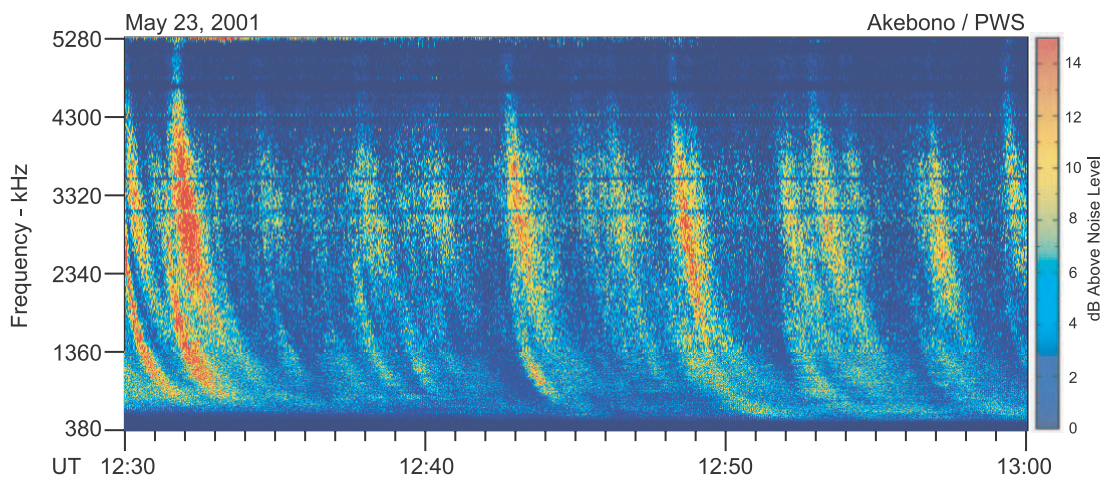


FIG. 6.—High time resolution (30 minute) dynamic spectrogram as observed by the *Akebono* satellite on 2001 May 23.

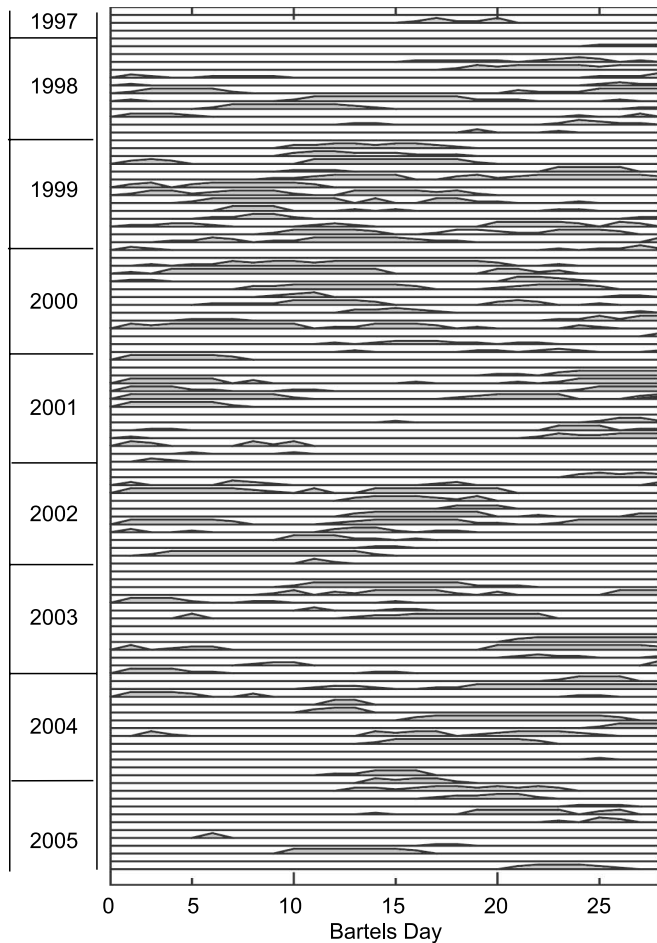


FIG. 7.—Diagram of the micro-type III index with respect to Bartels rotation for a period of 8 yr, from 1997 October 7 to 2005 November 23.

at shorter wavelengths and below  $3 \times 10^{-7} \text{ W m}^{-2}$  at longer wavelengths. This indicates that the micro-type III bursts are not accompanied by *GOES* soft X-ray activity.

## 5. RELATIONSHIP TO SOLAR ACTIVE REGIONS AND CORONAL HOLES

### 5.1. Development of Active Regions and Micro-Type III Bursts

The development of micro-type III bursts and their relation to active regions were examined in detail by using SolarMonitor data. Figure 10a shows the compressed 8 day dynamic spectrogram in the 80–50 kHz frequency range obtained by *Geotail* from 2004 March 7 to 14. Faint but continuous micro-type III bursts are seen above 100 kHz on March 7. On March 9 the burst intensity becomes enhanced, and this continues until March 12. Note that intense AKR (shown in yellow in the spectrogram) was observed intermittently in a wide frequency band from about 500 to 50 kHz from March 9 onward. The activation of AKR resulted from a geomagnetic storm that occurred on March 9 and continued until March 15, which was found to be independent of the continuous micro-type III bursts that occurred during this period. After March 13, the continuous micro-type III burst emission decreased. Figure 10b illustrates the daily magnetic field as seen by the Michelson Doppler Imager (MDI) on the *Solar and Heliospheric Observatory (SOHO)*. The magnetic field data show that only one active region, identified as NOAA AR 10570, was pres-

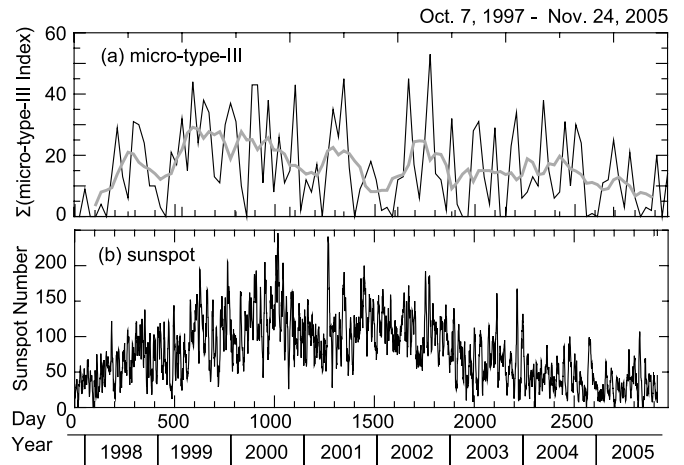


FIG. 8.—Relationship between (a) activity of micro-type III bursts as given by  $\sum$  mt-III (see text for definition) and (b) sunspot number during the period from 1997 to 2005. The gray line in (a) shows a running average of the  $\sum$  mt-III index.

ent on the solar disk during the period of interest. The active region grew day by day, and the sunspot area expanded. Figure 10c shows the daily variation in sunspot number in the active region. The stepwise increase in sunspot number on March 9 coincides with the enhancement of the micro-type III bursts, and the decay in sunspot number from March 13 onward coincides with the decrease in the burst activity. Figure 10d shows an image in the extreme-ultraviolet (Fe xv, 284 Å) from the *SOHO* EUV Imaging Telescope (EIT) on March 11, indicating that the active region bordered on a coronal hole.

Another example is shown in the compressed 12 day dynamic spectrogram from 2002 August 5–16 in Figure 11b. The format is the same as in Figure 10a. During this period, *Geotail* was located almost in interplanetary space, except for August 8 and 13. The emission bands seen below 100 kHz are local Langmuir waves that are excited near Earth's bow shock. The intense emissions (shown in yellow in the spectrogram) on August 13 are AKR. Ordinary type III bursts whose frequency extended below 100 kHz were detected intermittently during this period. Faint but continuous micro-type III bursts appeared above 100 kHz on August 7 and increased in intensity until August 13. Later on August 13, the continuous burst emission was found to have ceased. Figures 11c and 11d show *SOHO* MDI and EIT images for every third day, respectively. The magnetic field data show that only the large active region NOAA AR 10061 (circled) consistently accompanied the micro-type III burst group during this half-rotation of the Sun. Thus, NOAA AR 10061 is the region responsible for the micro-type III bursts. The top panel of Figure 11 shows the daily variation of sunspot number in NOAA AR 10061, which illustrates that the enhancement from August 7 to 13 corresponds to micro-type III activity. It should also be noted that there were large active regions on the solar disk after the decline of NOAA AR 10061 (see Figs. 11c and 11d for August 15). However, there was no micro-type III burst activity after August 14. This suggests that micro-type III bursts are not always related to large active regions but are preferentially radiated from particular active regions. An apparent feature of the active regions that are related to micro-type III bursts is their coincidence with coronal holes (Fig. 11d). The active region NOAA AR 10061 bordered on a coronal hole, as shown by the dotted circles, while the other large active regions seen on August 15 were not accompanied by coronal holes.

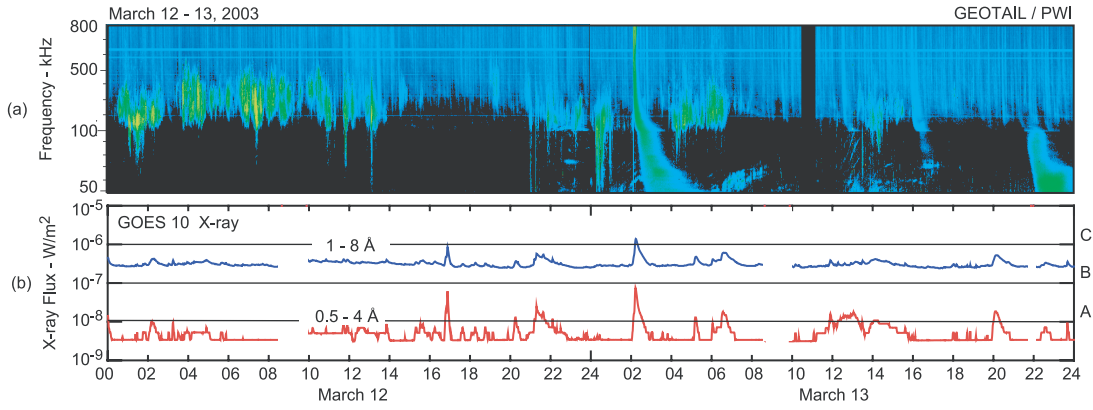


FIG. 9.—(a) Dynamic spectrogram of micro-type III bursts for a period of 2 days from 2003 March 12 to 13; (b) simultaneous *GOES 10* X-ray data at 1–8 Å (blue line) and 0.5–4 Å (red line).

5.2. Active Regions Bordering on Coronal Holes

It is noteworthy that the active regions in the examples above were located very close to coronal holes, as seen in the EIT images (Figs. 10d and 11d). This implies that the active regions responsible for the continuous micro-type III bursts might be characterized by their lying at the edges of coronal holes. Keeping this in mind, we have examined the relationship between those active regions responsible for continuous micro-type III bursts and their location with respect to coronal holes. Micro-type III burst events that continued for more than 8 days (more than a quarter of a solar rotation) were investigated during the declining phase of solar activity (2002 to 2005). We picked 11 such events for which both SolarMonitor and *Geotail* data were available. The active regions responsible for these events and their locations with respect to coronal holes were then investigated. The results are listed in

Table 1, which shows that eight of the 11 active regions were located at the edge of a coronal hole and that the remaining three were located next to regions where the coronal temperature was low but had not fully developed into a coronal hole. Based on this, we suggest that a necessary condition for an active region to emanate micro-type III bursts is that it border on a coronal hole. Contrary to our result, earlier work by Kayser et al. (1987, 1988) based on *ISEE 3* observations reported that most of the foot-points of type III storms were found to lie near active regions that did not coincide with coronal holes.

5.3. Coexistence of Ordinary Type III Bursts and Micro-Type III Bursts within an Active Region

It is a very interesting issue whether a single active region can radiate both continuous micro-type III and ordinary type III

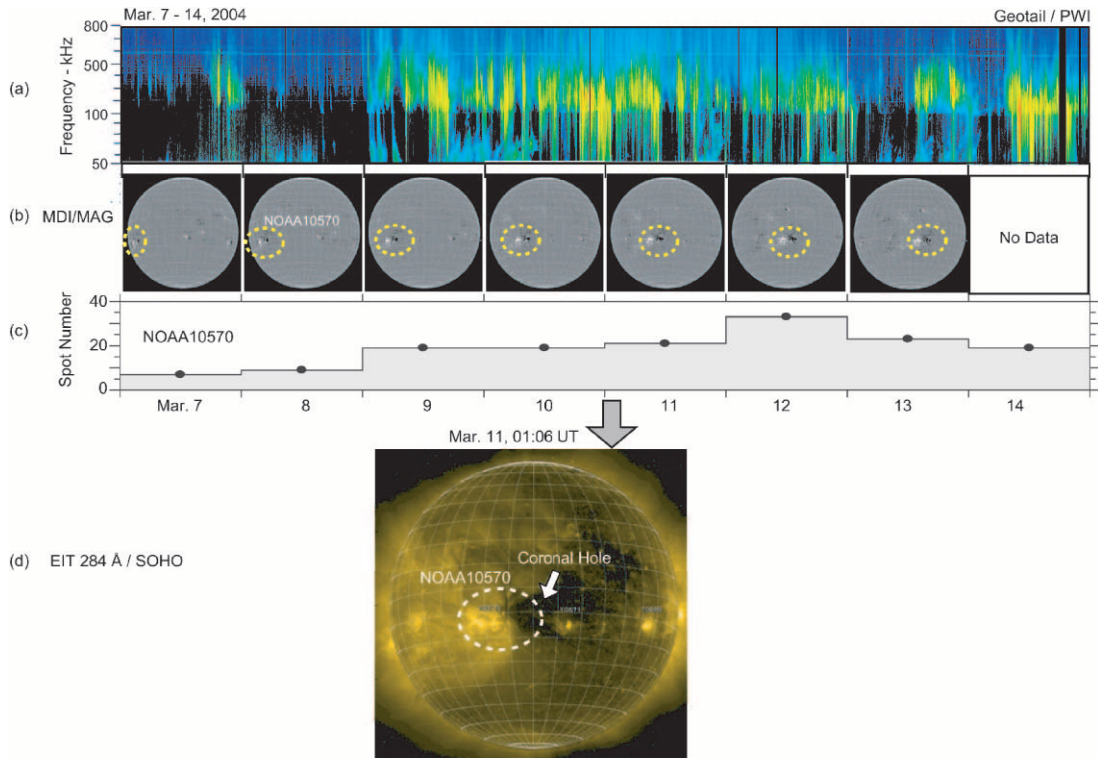


FIG. 10.—(a) Dynamic spectrogram for a period of 8 days from 2004 March 7 to 14. The spectra shown in blue above ~100 kHz are the micro-type III bursts. (b) Daily magnetograms (MDI) of the solar disk obtained from *SOHO* observations. The dotted circles indicate active region NOAA AR 10570. (c) Daily sunspot number for NOAA AR 10570. (d) EIT image (284 Å) from *SOHO* at 01:06 UT on March 11.

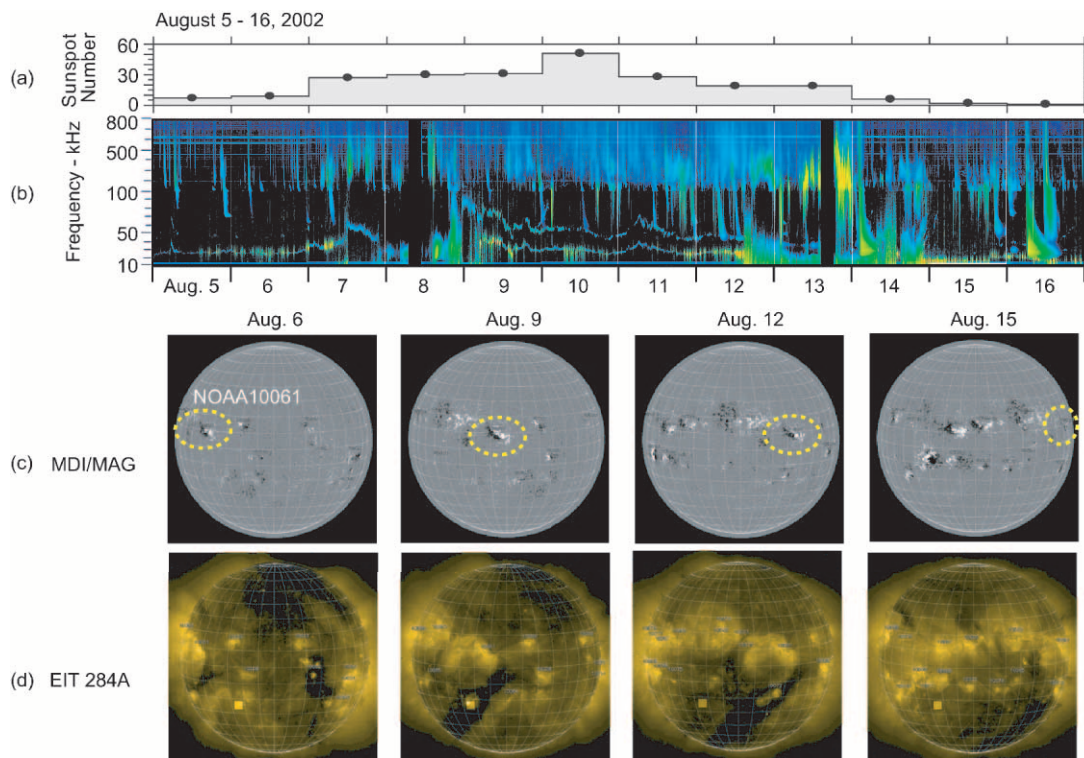


FIG. 11.—(a) Daily sunspot number in active region NOAA AR 10061. (b) Dynamic spectrogram for 12 days from 2002 August 5 to 16. (c) Daily magnetograms of the solar disk from *SOHO* observations. The dotted circles indicate NOAA AR 10061. (d) Daily EIT images (284 Å) from *SOHO* observations.

bursts or not, because we have inferred that their corresponding energy release processes are different (see Fig. 3). Figure 12a shows an example of a dynamic spectrogram in which many ordinary type III bursts seem to overlap continuous micro-type III bursts without any interference. Correspondingly, from Figures 12b and 12c it can be seen that there were two large active regions on the disk. We identified the region responsible for the continuous micro-type III bursts as NOAA AR 10484 by comparing the rise and fall of the active region from and into the solar limb with the corresponding appearance and disappearance of the burst group. Once again, it can be noted that the active region was located at the edge of a coronal hole. The active regions responsible for the ordinary type III bursts were also identified from the list of flares provided by NOAA. The ordinary type III bursts originating from NOAA AR 10484 are indicated with yellow triangles in Figure 12a. Thus, it can be seen that the same active region that radiated

continuous micro-type III bursts was also the source region for ordinary type III bursts. This indicates that an active region can produce two types of electron bursts whose acceleration processes are fairly different.

## 6. SUMMARY AND DISCUSSION

We have carried out a statistical analysis of the intensity distribution of micro-type III bursts, which are part of the so-called type III storms. The analysis shows that these are not just a weaker component of ordinary type III bursts but a different kind of emission, as shown by Figure 3. This indicates that the micro-type III bursts may not be directly related to microflares or transient brightenings, which have proved to be simple extensions or miniature versions of a general flare (e.g., Shimizu 1995; Aschwanden et al. 2000). This conclusion is moreover supported by evidence that the micro-type III bursts rarely correlate with the corresponding

TABLE 1  
MICRO-TYPE III BURSTS AND RELATED ACTIVE REGIONS INVESTIGATED IN THIS STUDY

No.	YEAR	BARTELS NUMBER	BURST START AND STOP DATES	CORRESPONDING ACTIVE REGION		CORRESPONDENCE TO CORONAL HOLE (CH)
				NOAA	Rise and Fall Dates	
1.....	2002	2303	Apr 10–20	09906	Apr 9–22	Bordered on CH
2.....	2002	2306	Jul 25–Aug 2	10044	Jul 24–Aug 4	Bordered on unclear CH
3.....	2002	2307	Aug 6–13	10061	Aug 5–16	Bordered on CH
4.....	2002	2311	Nov 14–25	10197	Nov 14–27	Bordered on CH
5.....	2003	2315	Mar 10–19	10311	Mar 10–19	Bordered on CH
6.....	2003	2316	Apr 4–15	10330	Apr 4–16	Bordered on CH
7.....	2003	2319	Jun 30–Jul 8	10397	Jun 27–11	Bordered on CH
8.....	2003	2323	Oct 20–28	10484	Oct 19–31	Bordered on CH
9.....	2004	2328	Mar 6–16	10570	Mar 5–19	Bordered on CH
10.....	2004	2335	Sep 3–12	10667	Sep 3–14	Bordered on unclear CH
11.....	2005	2341	Feb 11–21	10733	Feb 11–23	Bordered on unclear CH

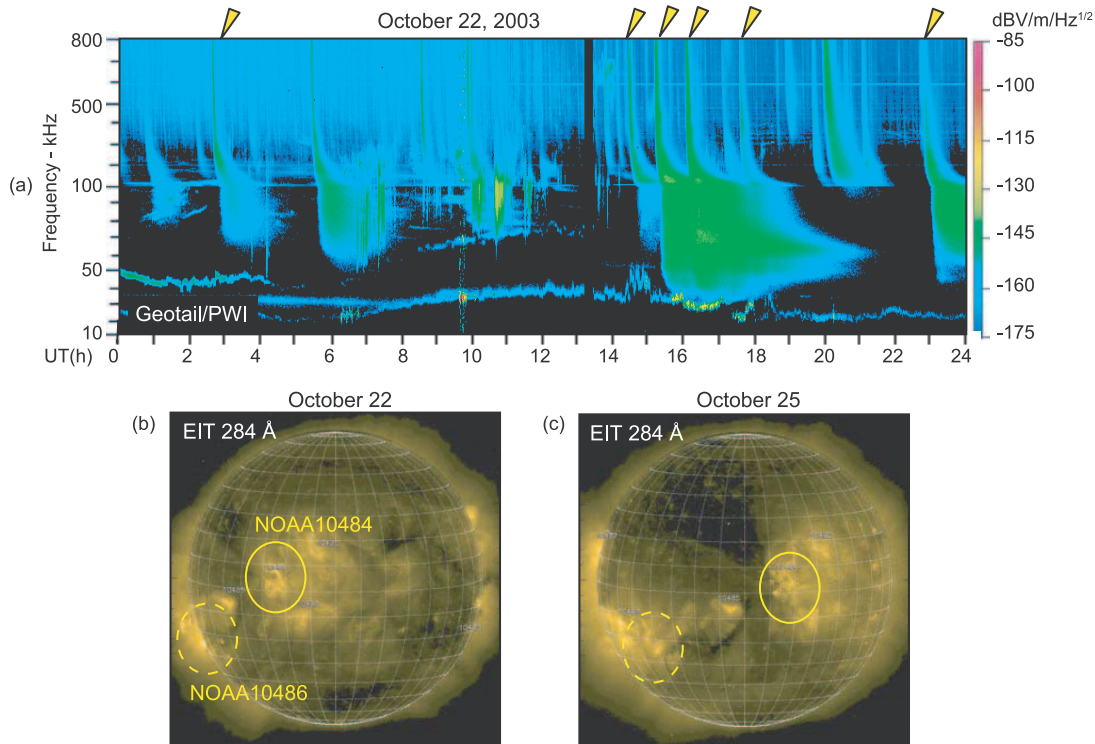


FIG. 12.—(a) Dynamic spectrogram for 2003 October 22. The triangles indicate ordinary type III bursts originating from the active region NOAA AR 10484. (b) Corresponding EIT image (284 Å) for October 22. The solid and dotted circles indicate active regions NOAA AR 10484 and 10486, respectively. (c) EIT image (284 Å) for October 25.

variation in total solar soft X-ray flux, as shown in Figure 9, whereas microflares are associated with X-ray events (class A/B in the *GOES* nomenclature) (Shimizu et al. 1992). Liu et al. (2004) showed that microflares are associated with type III bursts. However, the associated burst shown in Figure 4 of Liu et al. (2004) was not a micro-type III but an ordinary type III burst. Thus, it can be concluded that the micro-type III bursts belong to a different and much smaller category of energetic phenomena as compared with microflares.

It is very interesting that the micro-type III bursts have a rather constant cutoff frequency, which never extends below 100 kHz. As shown in Figure 1f, the cutoff frequencies of thousands of micro-type III bursts were almost constant for 2 hours, whereas their amplitudes varied. A plasma frequency of 100 kHz corresponds to a radial distance of about  $50 R_{\odot}$  according to the interplanetary plasma density model of Leblanc et al. (1998). One possible explanation for this peculiar feature may be that the weak electron beams injected into interplanetary space are already dispersed by  $50 R_{\odot}$  and the beam plasma instability that is responsible for the excitation of plasma waves ceases to function correspondingly. Based on *ISEE 3* measurements, Lin (1985) argued that the apparently impulsive injection of electrons is so frequent in a “type III storm” that the fluxes from individual injections are washed out by the time they reach 1 AU. If these beams are dispersed by  $50 R_{\odot}$ , as in the case of micro-type III bursts, the corresponding cutoff frequency for the excited type III bursts would be around 100 kHz. A problem with this explanation, however, is that the cutoff frequencies for micro-type III bursts appear to be almost constant for long periods of time despite changes in their amplitudes (as seen in Figs. 1c and 1d). Another possible explanation may be that the electron beams that excite micro-type III bursts are trapped in closed field lines that extend to  $\sim 50 R_{\odot}$ . Nearly constant cutoff frequencies for long

periods of time would indicate a rather steady closed magnetic field configuration above the active region. However, this hypothesis contradicts the arguments of Bougeret et al. (1984a) and Lin (1985), in which the so-called type III storms are believed to be associated usually with long-lived streams of electrons at a distance of 1 AU. In the near future, it will be important to investigate the relationship between in situ solar electron beams and remote micro-type III bursts with a combination of *Akebono/Geotail* and *ACE/Wind* data.

We have demonstrated that both ordinary type III and micro-type III bursts can be emitted from the same active region. Besides, the ejection of a powerful ordinary type III burst does not affect continuous micro-type III bursts that are preexisting. The mutually exclusive nature of these two types of bursts suggests that their energy storage and release mechanisms are quite different and independent from one another.

Another important feature, aside from the low intensity of micro-type III bursts, is that they are continuous during the period of enhancement of the active region. This suggests that certain continuous energy storage and release processes are at work, independently of the considerably larger energy release processes associated with flares in the highly active region. This coupling of “weak intensity” with “long duration” could be an important key to understanding constant electron beam acceleration processes.

The relationship between micro-type III bursts and metric type III and/or type I storms would provide helpful information on the acceleration processes of nonthermal electrons (Fainberg & Stone 1970a). The correlation study that first related them was carried out by Bougeret et al. (1984a), who claimed that the electrons responsible for interplanetary storms (micro-type III bursts), metric type III storms, and type I storms are accelerated at heliocentric altitudes below  $1.5 R_{\odot}$ . The recent observations of metric

and decimetric solar radio noise storms, in combination with data from the *SOHO*, *TRACE*, and *Wind* solar missions, have advanced the discussion of the source dynamics and electron acceleration processes (see, e.g., Willson 2002 and references therein). By combining the kilo-/hctometric observations made by the *Geotail* and *Akebono* spacecraft with the metric observations from solar observatories, a comprehensive and detailed analysis of such storms (metric and kilo-/hctometric) would be possible. This would lead to a better understanding of the acceleration and propagation of nonthermal electrons and their source structure around active regions.

The SolarMonitor Data were provided by NASA Goddard Space Flight Center's Solar Data Analysis Center. These data contain archived information on active regions and solar activity, using data from the Global H-alpha Network, ESA/NASA's *Solar and Heliospheric Observatory*, and the National Oceanic and Atmospheric Administration (NOAA). The Solar Event Lists and *GOES* 5 minute X-ray data were provided courtesy of the Space Environment Center, NOAA, US Department of Commerce. The Nobeyama Radio Heliograph data were provided courtesy of the Nobeyama Radio Observatory, National Astronomical Observatory of Japan.

## REFERENCES

- Aschwanden, M. J., Tarbell, T. D., Nightingale, R. W., Schrijver, C. J., Title, A., Kankelborg, C. C., Martens, P., & Warren, H. P. 2000, *ApJ*, 535, 1047  
 Bougeret, J.-L., Fainberg, J., & Stone, R. G. 1984a, *A&A*, 136, 255  
 ———. 1984b, *A&A*, 141, 17  
 Dulk, G., Leblanc, Y., Robinson, P. A., Bougere, J.-L., & Lin, R. P. 1998, *J. Geophys. Res.*, 103, 17223  
 Ergun, R. E., et al. 1998, *ApJ*, 503, 435  
 Fainberg, J., & Stone, R. G. 1970a, *Sol. Phys.*, 15, 222  
 ———. 1970b, *Sol. Phys.*, 15, 433  
 ———. 1971, *Sol. Phys.*, 17, 392  
 ———. 1974, *Space Sci. Rev.*, 16, 145  
 Gurnett, D. A., & Anderson, R. R. 1976, *Science*, 194, 1159  
 Hudson, H. S. 1991, *Sol. Phys.*, 133, 357  
 Kayser, S. E., Bougeret, J.-L., Fainberg, J., & Stone, R. G. 1987, *Sol. Phys.*, 109, 107  
 ———. 1988, *A&AS*, 73, 243  
 Klein, K.-L., Krucker, S., Trotter, G., & Hoang, S. 2005, *A&A*, 431, 1047  
 Leblanc, Y., Dulk, G. A., & Bougeret, J.-L. 1998, *Sol. Phys.*, 183, 165  
 Lin, R. P. 1985, *Sol. Phys.*, 100, 537  
 Lin, R. P., Potter, D. W., Gurnett, D. A., & Scarf, F. L. 1981, *ApJ*, 251, 364  
 Lin, R. P., Schwartz, R. A., Kane, S. R., Pelling, R. M., & Hurley, K. C. 1984, *ApJ*, 283, 421  
 Liu, C., Qui, J., Gary, D. E., Krucker, S., & Wang, H. 2004, *ApJ*, 604, 442  
 Matsumoto, H., et al. 1994, *J. Geomagn. Geoelectricity*, 46, 59  
 Ogawara, Y., Takano, T., Kato, T., Kosugi, T., Tsuneta, S., Watanabe, T., Kondo, I., & Uchida, Y. 1991, *Sol. Phys.*, 136, 1  
 Oya, H., Morioka, A., Kobayashi, K., Iijima, M., Ono, T., Miyaoka, H., Okada, T., & Obara, T. 1990, *J. Geomagn. Geoelectricity*, 42, 411  
 Porter, J. G., Fontenla, J. M., & Simnett, G. M. 1995, *ApJ*, 438, 472  
 Porter, J. G., Moore, R. L., Reichmann, E. J., Engvold, O., & Harvey, K. L. 1987, *ApJ*, 323, 380  
 Reiner, M. 2001, *Space Sci. Rev.*, 97, 129  
 Shibata, K., et al. 1992, *PASJ*, 44, L173  
 Shimizu, T. 1995, *PASJ*, 47, 251  
 Shimizu, T., Tsuneta, S., Acton, L. W., Lemen, J. R., Ogawara, Y., & Uchida, Y. 1994, *ApJ*, 422, 906  
 Shimizu, T., Tsuneta, S., Acton, L. W., Lemen, J. R., & Uchida, Y. 1992, *PASJ*, 44, L147  
 Simnett, G. M. 2005, *Sol. Phys.*, 229, 213  
 Wild, J. P., Smerd, S. F., & Weiss, A. A. 1963, *ARA&A*, 1, 291  
 Willson, R. 2002, *Sol. Phys.*, 211, 289